

Theory of Rapid Excitation-Energy Transfer from B800 to Optically-Forbidden Exciton States of B850 in the Antenna System LH2 of Photosynthetic Purple Bacteria

Koichiro Mukai,[†] Shuji Abe,* and Hitoshi Sumi^{‡,§}

Electrotechnical Laboratory, 1-1-4 Umezono, Tsukuba 305-8568, Japan, and Institute of Materials Science, University of Tsukuba, Tsukuba 305-8573, Japan

Received: November 18, 1998

Excitation-energy transfer (EET) has been observed to be very rapid from B800 to B850, between two circular aggregates of bacteriochlorophyll molecules (BChls), in the light-harvesting antenna complex LH2 of photosynthetic purple bacteria. This rapid EET cannot be understood within the framework of Förster's formula, since the luminescence spectrum of B800 overlaps little with the absorption spectrum of B850. The present work shows that it can be rationalized on the basis of a recently proposed formula for EET between molecular aggregates. The formula differs from Förster's one when excited states are excitonic at least in one of the donor and the acceptor aggregates with a mutual distance not much larger than their physical sizes, as in the present case. Excited states of B850 are regarded as excitonic, while those of B800 as monomeric. The exciton–phonon coupling was taken into account over all orders for B800 and within a self-consistent second-order perturbation for B850. Calculated rates of the EET are in the range of 10^{11} – 10^{12} s^{−1}, increasing weakly with temperature, in good agreement with experiments. We demonstrate that this rapid EET occurs to optically forbidden exciton states of B850, without total transition dipole, due to strong interaction of a transition dipole on a BChl in B800 with those on nearby BChls in B850.

1. Introduction

Recently much attention has been aroused on initial electronic processes of photosynthesis since the discovery of beautiful three-dimensional arrangements of pigments in the reaction center^{1,2} and the antenna system^{3,4} protein matrix of photosynthetic purple bacteria. Photosynthesis in purple bacteria⁵ starts from light harvesting by the peripheral antenna system called LH2 and subsequent excitation-energy transfer (EET) to the core antenna system LH1, which is believed to encircle the reaction center. The LH2 is composed of an inner ring of closely packed bacteriochlorophyll molecules (BChls) and an outer ring of loosely packed BChls.^{3,4} They are called B850 and B800, respectively, after the wavelengths of characteristic Q_y absorption peaks around 850 and 800 nm.

EET takes place also within the LH2, from B800 to B850.⁵ Time-resolved spectroscopy has revealed that this EET is very rapid with a time constant of less than 1 ps at room temperature.^{6,7} This rapid EET cannot be rationalized on the basis of Förster's formula⁸ because of very small overlap between the luminescence spectrum of B800 and the absorption spectrum of B850. It would predict a rate constant as slow as about 20 ns.⁷ In fact, the spectral width (full width at half-maximum) of the B850 absorption peak (at $\sim 11\,475$ cm^{−1}) is ~ 320 cm^{−1} at room temperature and ~ 200 cm^{−1} at 4.2 K, and that of B800 (at $\sim 12\,440$ cm^{−1}) is ~ 240 cm^{−1} at room temperature and ~ 130 cm^{−1} at 4.2 K⁹ in *Rhodospseudomonas acidophila*. The widths of these peaks are partially due to inhomogeneous broadening, while homogeneous widths and phonon sidebands have also

been observed in hole-burning and site-selective fluorescence experiments.^{10,11} The EET slows down weakly with lowering temperatures. The time constant of 2.4 ps at 4 K has been obtained by hole-burning experiments,^{10,11} with variations of 1.5 ps at 4.2 K¹² and 1.2 ps at 77 K^{12,13} by time-domain experiments. Such a weak temperature dependence also cannot be understood within the framework of Förster's formula, which would predict a much stronger temperature dependence due to substantial decrease of the spectral overlap with lowering temperature.

It will be shown in the present work that this rapid EET can be rationalized on the basis of a new formula recently proposed by one of the authors.¹⁴ This formula differs from Förster's one when excited states are excitonic at least in one of the donor and the acceptor aggregates with a mutual distance not much larger than their physical sizes. In this situation, this formula correctly describes that EET takes place rapidly also to and/or from optically forbidden exciton states, without total transition dipole, due to strong interaction between a transition dipole on a molecule in the donor and those on nearby molecules in the acceptor (and vice versa). We demonstrate that this rapid EET observed is a concrete example, occurring to optically forbidden exciton states in B850 which are broadened due to phonon coupling.

2. Formula for EET between Molecular Aggregates

In light-harvesting processes of photosynthesis, EET often takes place between aggregates of chromophores,¹⁴ as seen in the EET from B800 to B850. This situation plays important roles in EET, when the distances between the donor and the acceptor aggregates are not much larger than their physical sizes.^{14,15}

* Corresponding author. E-mail: abe@etl.go.jp.

[†] E-mail: evemk@etl.go.jp.

[‡] E-mail: sumi@ims.tsukuba.ac.jp.

[§] University of Tsukuba.

According to the new formula for EET between molecular aggregates in the situation mentioned above,¹⁴ the rate constant of EET is given by

$$\kappa = \frac{2\pi}{\hbar} \int dE \text{Tr}^{(D)} \mathbf{W}_{A,D} \cdot \mathbf{I}^A(E) \cdot \mathbf{W}_{A,D} \cdot \mathbf{L}^D(E) \quad (1)$$

when the donor and the acceptor are respectively composed of M_D and M_A molecules. Here, $\mathbf{W}_{A,D}$ is an $M_A \times M_D$ matrix whose ij component represents the electrostatic interaction between transition dipoles on the i th molecule in the acceptor (A) and the j th one in the donor (D). As explained below, $\mathbf{L}^D(E)$ and $\mathbf{I}^A(E)$ represent an M_D - and an M_A -dimensional square matrices spanned by electronic excited states in the donor and the acceptor, respectively. $\text{Tr}^{(D)}$ implies taking a trace over electronic excited states in the donor. Matrix multiplication denoted by \cdot can be performed on any basis set of excited states in the donor or the acceptor, including exciton states therein.

Exciton states in each aggregate are given by a linear combination of excited states of individual molecules. On the basis of the exciton states, $\mathbf{W}_{A,D}$ represents the interaction between the exciton states in the donor and those in the acceptor, being given by appropriate linear combinations of the intermolecular transition-dipole interactions. $\mathbf{I}^A(E)$ represents the density of exciton states in the acceptor, defined under thermal averaging over phonons in the ground state. It is given by the imaginary part of the retarded Green's function for exciton: for the k', k element,

$$I_{k'k}^A(E) = -\frac{1}{\pi} \text{Im} G_{k'k}(E) \quad (2)$$

where

$$G_{k'k}(E) = \int \tilde{G}_{k'k}(t) e^{iEt/\hbar} dt/\hbar \quad (3)$$

$$\tilde{G}_{k'k}(t) = -i\theta(t) \langle a_{k'}(t) a_k^\dagger(0) \rangle_{\text{av}} \quad (4)$$

Here, $a_k(t)$ represents the time evolution of the annihilation operator a_k of an exciton at the k th state in the acceptor, defined by

$$a_k(t) = \exp(iHt/\hbar) a_k \exp(-iHt/\hbar) \quad (5)$$

where H represents the Hamiltonian for the exciton-phonon system in the acceptor. The averaging $\langle \dots \rangle_{\text{av}}$ in eq 4 is taken over phonons in the exciton vacuum, and $\theta(t)$ represents the step function equal to 1 for $t > 0$ and 0 for $t < 0$. $\mathbf{I}^A(E)$ is normalized as

$$\int dE \text{Tr}^{(A)} \mathbf{I}^A(E) = M_A \quad (6)$$

where $\text{Tr}^{(A)}$ represents taking a trace over electronic excited states in the acceptor which contains M_A molecules. $\mathbf{L}^D(E)$ is related to $\mathbf{I}^D(E)$ defined similarly to $\mathbf{I}^A(E)$, as

$$\mathbf{L}^D(E) = B e^{-\beta E} \mathbf{I}^D(E) \quad (7)$$

with $\beta = (k_B T)^{-1}$, and B is a constant determined by the normalization

$$\int dE \text{Tr}^{(D)} \mathbf{L}^D(E) = 1 \quad (8)$$

$\mathbf{L}^D(E)$ represents the density of exciton states under a condition that excitons are annihilated from the donor, defined by thermal averaging over phonons in the electronic excited states.

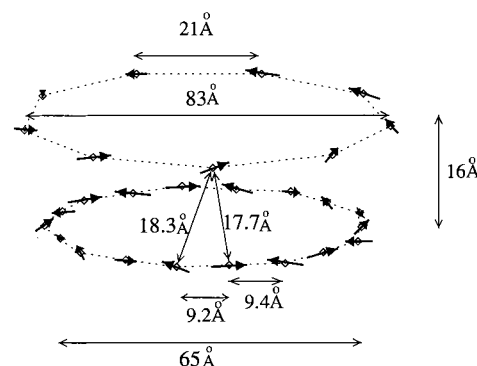


Figure 1. Schematic illustration of the arrangement of the Q_y transition dipoles of BChls in the B850 (lower) and B800 (upper) rings.

The dipole-dipole interaction between individual molecules in $\mathbf{W}_{A,D}$ depends on both the mutual distance and orientation between two transition dipoles. When the distance between the donor and the acceptor aggregates is not much larger than their physical sizes, the image of individual molecules in the acceptor seen by a molecule in the donor, through this interaction, significantly varies depending on their location and orientation within the acceptor, and vice versa. Especially, molecules in the acceptor near from the molecule in the donor are seen more largely than other molecules in the acceptor. In this situation, the interaction between the donor and the acceptor cannot be approximated by that between their total transition dipoles, only what is regarded as causing EET in Förster's theory. This feature is correctly taken into account in eq 1 such that EET can take place between any pair of exciton states in the donor and the acceptor, irrespective of whether they are optically allowed or forbidden, because of the large distance and orientation dependence of individual dipole-dipole interactions in $\mathbf{W}_{A,D}$. When the distance between the aggregates is much larger than their physical sizes, on the other hand, the matrix elements of $\mathbf{W}_{A,D}$ other than that between optically allowed states tend to vanish, and eq 1 reduces to Förster's formula.¹⁴

3. Exciton-Phonon Interactions and EET in LH2

3.1. Hamiltonian for the B850 Ring. In the antenna system from *Rps. acidophila*, the LH2 complex consists of nine units, each of which contains three BChl *a* molecules (one for B800 and two for B850) together with a carotenoid (rhodospinglucoside).¹⁶ These chromophores are noncovalently bound by two short apoproteins in a single unit. The LH2 can be regarded as having a 9-fold rotational symmetry. Positions and orientations of BChls are weakly alternating in the B850 ring (e.g., the Mg-to-Mg distance is 9.4 Å within a dimer and 9.2 Å between adjacent dimers).¹⁶

In another species of purple bacteria, *Rhodospirillum molischianum*, the basic structure in the arrangement of chromophores is similar, but the LH2 consists of eight units rather than nine.⁴ Although we focus mainly on *Rps. acidophila* in the following, the basic idea and the calculation method of the present work can be applied also to other species such as *Rs. molischianum*, for which we expect similar results.

The nature of electronic excited states in B850 has been a subject of discussions. The close packing of the BChls leads to a fairly large nearest-neighbor coupling ($\geq 300 \text{ cm}^{-1}$)¹⁷⁻¹⁹ between the Q_y molecular excitations, whose transition dipole moments are arranged almost tangentially along the ring, as shown in Figure 1. Therefore, it is natural to describe excited states in the B850 ring as excitons. A number of investigators

have taken this standpoint,^{17,20–23} while others have claimed localization of the excited states due to disorder.^{24–27}

The present work is based on the exciton model for B850, which will turn out to be essential in reproducing the observed EET rates as shown below. In the case of B800, the distance between adjacent BChls is about 21 Å,¹⁶ indicating a fairly weak coupling between them. Therefore, we treat the B800 BChls as a collection of independent monomers (see section 3.3). The electronic excitation on each chromophore interacts with distortions of surrounding proteins. This is the origin of the exciton–phonon interaction in the present system. We introduce a model Hamiltonian for the exciton–phonon system in the B850 ring composed of $2N$ BChls, as

$$H = H_e + H_{ph} + H' \quad (9)$$

with

$$H_e = \sum_n E_n a_n^\dagger a_n + \sum_{m,n(m \neq n)} J_{mn} a_m^\dagger a_n \quad (10)$$

$$H_{ph} = \sum_i (\nu_i \sum_n b_n^{(i)\dagger} b_n^{(i)}) \quad (11)$$

$$H' = \sum_i [\sqrt{S_i} \nu_i \sum_n a_n^\dagger a_n (b_n^{(i)\dagger} + b_n^{(i)})] \quad (12)$$

H_e is the Hamiltonian for excitons with the Q_y excitation energy E_n of a BChl at each site n ($=1, 2, \dots, 2N$) and their coupling J_{mn} between the m th and n th BChls. a_n and a_n^\dagger are annihilation and creation operators of an exciton at the n th site. J_{mn} is assumed to be given by the electrostatic interaction between transition dipoles μ_m and μ_n on these BChls as

$$J_{mn} = \frac{1}{\epsilon} \left[\frac{\mu_m \cdot \mu_n}{|\mathbf{R}_{mn}|^3} - \frac{3(\mu_m \cdot \mathbf{R}_{mn})(\mu_n \cdot \mathbf{R}_{mn})}{|\mathbf{R}_{mn}|^5} \right] \quad (13)$$

where \mathbf{R}_{mn} is the spatial vector connecting the centers of the m th and n th molecules, and ϵ is the dielectric constant of the LH2 protein–chromophore complex. H_{ph} is the Hamiltonian for phonons arising from distortions of a protein matrix around each BChl. $b_n^{(i)}$ is the annihilation operator of a phonon of the i th mode with energy ν_i around the n th BChl. Phonon modes around a BChl are assumed to be independent of those around a different BChl, possessing the same continuous spectrum of ν_i . H' describes interactions between an exciton and phonons around each BChl. S_i is the coupling constant (called the Huang–Rhys factor) defined for each phonon mode and assumed to be independent of the site index n . Modulations of the electronic coupling J_{mn} by phonons are neglected in the present model.

Positions of the BChls in LH2 are chosen at those for *Rps. acidophila*, being taken from the protein data bank.¹⁶ In this case, N equals 9. We take the Q_y transition dipole of a BChl as located at the Mg atom in the chlorin macroring and directed along a line connecting two N atoms on the pyrrol rings I and III of BChl. Figure 1 illustrates the arrangement of the dipole moments, which are approximately in-plane and tangential in both the B800 and B850 rings.

In the present work, static disorder is neglected in both E_n 's and J_{mn} 's, and E_n 's are regarded as independent of the site index n , being given by E_0 . In this case, the Hamiltonian H of eq 9 has an N -fold rotational symmetry. Diagonalization of the unperturbed Hamiltonian H_e leads to delocalized exciton states with energy levels displayed in Figure 2. We use an index k to

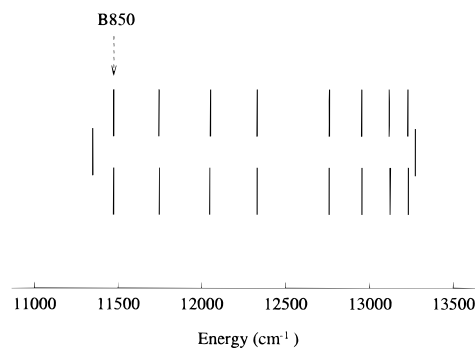


Figure 2. Calculated exciton energy levels in the B850 ring.

specify the exciton levels as $k = 0, \pm 1, \pm 2, \dots, \pm(N-1)$, N in the order of increasing energy (the states with k and $-k$ are degenerate). Accordingly, the Hamiltonian can be rewritten as

$$H_e = \sum_k E_k a_k^\dagger a_k \quad (14)$$

We use cyclic labels such that the index k is identified in the period of $2N$, i.e., $a_{k+2N} = a_k$. The index k would represent the angular momentum or the wavenumber concerned with rotation around the ring if our system had a $2N$ ($=18$)-fold rotational symmetry. In the present case of the reduced N -fold symmetry, we still use the same index and call it (angular) wavenumber. This does not mean that we have assumed the $2N$ -fold rotational symmetry. k for $|k| > N/2$ is simply a mathematical expediency for indexing the exciton states. (Actually, it corresponds to the wavenumber shifted by a constant N when $|k| > N/2$.)

If we take into account only the in-plane component of the total transition dipole, practically only the $k = \pm 1$ exciton states have nonvanishing transition dipole moments. All the other k states are dipole-forbidden, although the states for $k = \pm(N-1)$ have very small transition dipoles. These general features of excitons in circular antenna systems have been discussed previously by many investigators.^{5,7,17,18}

We adopt the parameters $\epsilon = 1$ and $|\mu_n| = 7.3$ debye to calculate interactions J_{mn} by eq 13. In this case the nearest-neighbor coupling $J_{n,n+1}$ is about 540 cm^{-1} within a dimer and 380 cm^{-1} between adjacent dimers. These interaction strengths are larger than an estimation from the monomer absorption in solution,¹⁷ but is smaller than a theoretical estimation.²⁸ The above set of parameters reproduces the optically allowed level ($k = \pm 1$) of B850 observed at $11\,475 \text{ cm}^{-1}$ without invoking a monomer shift, i.e., simply by assuming that the molecular excitation energy E_0 of B850 is the same as that of the B800 monomer observed at $12\,440 \text{ cm}^{-1}$. This is a reason why we have chosen those parameters.

There is experimental evidence supporting this choice. In a hole-burning experiment, zero-phonon holes have been observed on the low-energy side of B850,^{20,29} centered at 885 nm ($11\,300 \text{ cm}^{-1}$). Analogous holes have been observed also in the LH1 and LH2 from *Rhodobacter sphaeroides*.³⁰ The circular dichroism spectra display a negative band around 885 nm .^{18,31,32} These features have been ascribed to the dipole-forbidden, lowest exciton level ($k = 0$) of B850. In Figure 2, the calculated lowest exciton level is located at $11\,340 \text{ cm}^{-1}$, which agrees with those experiments.

3.2. Green's Function for Exciton. The exciton–phonon interaction gives rise to the self-energy of Green's function.³³ As will be shown later in the Appendix, the self-energy is approximated as independent of the wavenumber k , depending only on the energy variable E , written as $\Sigma(E)$, in the second

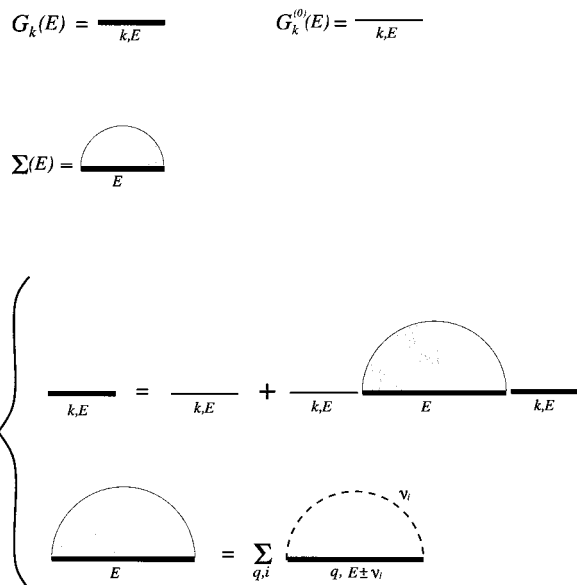


Figure 3. Diagrammatic representation of the self-consistent second-order calculation for the self-energy of Green's function.

order approximation in the interaction. In this case, in the total Hamiltonian H of eq 9, the interaction H' is regarded as giving rise to the same energy shift, by $\Sigma(E)$, of the electronic excitation energy at any molecule in the B850 ring in the unperturbed Hamiltonian H_e of eq 10. In this situation, Green's function should be diagonalized by the same wavenumber k as diagonalizing H_e , i.e.

$$G_{kk}(E) = \delta_{kk'} G_k(E) \quad (15)$$

$I_k^{(\Lambda)}(E)$ is also diagonal in the wavenumber, and each of its diagonal elements, $I_k^A(E)$, represents the density of exciton states for a specific wavenumber k , given by

$$I_k^A(E) = -\frac{1}{\pi} \text{Im } G_k(E) \quad (16)$$

Taking the energy shift $\Sigma(E)$ into account, Green's function $G_k(E)$ is written as

$$G_k(E) = \frac{1}{E - E_k - \Sigma(E)} \quad (17)$$

Since exciton–phonon coupling constants deduced from experiments are fairly small as we will see in section 3.4, the self-energy can be calculated by the second-order perturbation (including its self-consistent version) with respect to the exciton–phonon interaction H' of eq 12. In general, the self-energy depends not only on the energy variable E but also on the wavenumber k , but in the present case it does not depend on k : As mentioned in section 3.1, the phonon modes around different BChls were assumed to be independent of each other. In this case, as long as the self-energy is calculated with the second-order perturbation theory including its self-consistent version, the self-energy is diagonal in the site representation and can be regarded as having the same value at every site (for more details, see Appendix). This means that it does not depend on k in the k representation.

In the self-consistent second-order perturbation theory for the self-energy, Green's function of eq 17 is calculated by Feynman diagrams in Figure 3. The thick and the thin line therein denote Green's functions for excitons propagating under H and H_e ,

respectively. The broken line denotes a propagator for phonons. In Figure 3 we have two relations between Green's function and the self-energy. The first one is equivalent to eq 17, and the second one expresses the self-energy in terms of propagators for excitons and phonons.

As shown in the Appendix, these two relations enable us to obtain a self-consistency equation for $\Sigma(E)$, explicitly written as

$$\Sigma(E) = \frac{C}{2N} \int d\nu \rho(\nu) \nu \sum_q \left(\frac{n_\nu(T)}{E - E_q + \nu - \Sigma(E + \nu)} + \frac{n_\nu(T) + 1}{E - E_q - \nu - \Sigma(E - \nu)} \right) \quad (18)$$

where C is the reorganization energy due to interaction with phonons at each BChl and $\rho(\nu)$ is the density of phonon states weighted by the Huang–Rhys factor and the phonon energy, given by

$$C = \sum_i S_i \nu_i \quad (19)$$

$$\rho(\nu) = C^{-1} \sum_i \delta(\nu - \nu_i) S_i \nu_i \quad (20)$$

$n_\nu(T)$ is the thermal occupation number for a phonon with energy ν at temperature T . The first and second terms in the parentheses on the right-hand side of eq 18 result from exciton-scattering processes with phonon absorption and emission, respectively. The total integration of $\rho(\nu)$ is normalized to unity.

3.3. Luminescence Spectrum of B800. The distance between adjacent BChls is about 21 Å in the B800 ring in contrast to less than 10 Å in the B850 ring. Therefore, electronic excited states in B800 can be regarded as monomeric. Since the donor state of the EET is localized on a single BChl in B800, $L^D(E)$ defined in eq 7 is not a matrix but a scalar quantity with only one component $L^D(E)$ given by the normalized luminescence spectrum of the BChl. Also this monomeric excitation interacts with distortions of a protein matrix around it in the same manner as in B850. By assuming a linear exciton–phonon coupling as in eq 12, the absorption spectrum is calculated exactly³⁴ as

$$I^D(E) = \int \exp \left[-i(E_0 - E)t/\hbar - \sum_i S_i \coth(1/2\beta\nu_i) + \sum_i \frac{S_i}{2} (1 + \coth(1/2\beta\nu_i)) e^{i\nu_i t/\hbar} - \sum_i \frac{S_i}{2} (1 - \coth(1/2\beta\nu_i)) e^{-i\nu_i t/\hbar} \right] dt/\hbar \quad (21)$$

where i indexes a phonon mode with energy ν_i and the Huang–Rhys factor S_i , and E_0 is the excitation energy of the B800 monomer, being set at 12 440 cm⁻¹ (804 nm in wavelength). Phonon energies are regarded as continuously distributed. Since the protein environment around a B800 BChl is different from that around a B850 BChl, the phonon energies and the Huang–Rhys factors for the donor can be different from those for the acceptor (vide infra).

The luminescence spectrum $L^D(E)$ is related to $I^D(E)$ by eqs 7 and 8, in the present case

$$L^D(E) = Be^{-\beta E} I^D(E) \quad (22)$$

$$\int dE L^D(E) = 1 \quad (23)$$

3.4. Phonon Spectral Functions. The weighted density $\rho(\nu)$ of phonon states can be derived from observed luminescence spectra of a BChl in the antenna systems.^{10,35} The impurity-center theory³⁶ relates $\rho(\nu)$ of eq 20 to the phonon sideband spectrum $\Phi(\nu)$ at low temperatures^{35–38} by

$$\alpha\rho(\nu) = \nu\Phi(\nu) - \int_0^\nu \Phi(\nu - \nu')\rho(\nu') d\nu' \quad (24)$$

where α is the relative intensity of the zero-phonon line in the absorption spectrum at 0 K, given by $\alpha = \exp(-S)$ with the use of the total Huang–Rhys factor $S = \sum_i S_i$.

Homogeneously broadened spectra of BChls in proteins have been obtained by site-selective fluorescence spectroscopy. At low temperatures, the luminescence spectrum of B800 is substantially asymmetric and its phonon sideband has a maximum at about 20–30 cm^{-1} .¹⁰ In the BChl dimer called B820, which is believed to have a structure similar to the unit dimer of B850, a phonon sideband has also been observed with a peak at $\sim 100 \text{ cm}^{-1}$.³⁵

On the basis of the spectral shapes of these phonon sidebands observed, we assume that $\Phi(\nu)$ has a simple form

$$\Phi(\nu) = \begin{cases} \nu \exp(-\nu/\mu), & \nu > 0 \\ 0, & \nu < 0 \end{cases} \quad (25)$$

where μ represents the peak energy of the phonon sideband. For B800, a fitting with the observed spectrum gives $\mu = 20 \text{ cm}^{-1}$. Since there is no experimental data on a monomer of B850, we borrow the data of the B820 dimer. This leads us to set μ at 100 cm^{-1} for B850. As for the total Huang–Rhys factor, $S = 0.3$ – 0.6 has been estimated, corresponding to small exciton–phonon interaction.^{11,39} Here we take $S = 0.3$ for both B800 and B850, which leads to $\alpha = 0.74$. Using these parameters, $\rho(\nu)$ for each of B800 and B850 was obtained by solving eq 24 numerically. Calculated results are shown in Figure 4, a and b, for B850 and B800, respectively. The spectral functions thus obtained were in turn used to calculate the self-energy for B850 by eq 18 and the spectrum $I^D(E)$ for B800 by eq 21.

3.5. Rates of EET from B800 to B850. As mentioned in sections 3.2 and 3.3, the matrix $I^A(E)$ for B850 is diagonal in the k representation, while $L^D(E)$ is replaced by the scalar $L^D(E)$ of the normalized luminescence spectrum of B800. In this case the formula of EET in eq 1 reduces to

$$\kappa = \frac{2\pi}{\hbar} \int dE \sum_k |W_k|^2 I_k^A(E) L^D(E) \quad (26)$$

Here W_k denotes the EET coupling of the localized excited state of a BChl in B800 with the exciton state of wavenumber k in B850. It is calculated by transforming the individual dipole–dipole interactions (of eq 13) with each BChl of B850 into that interaction with the exciton state k which is an appropriate linear combination of excited states of BChls in B850.

Figure 5 displays calculated rate constants of the EET from B800 to B850 as a function of temperature. Time constants obtained are ~ 3.4 ps for 77 K and ~ 1.5 ps for 300 K. These values are in good agreement with the experiments (1.2–2.5 ps at 77 K,^{12,13} and ~ 0.7 ps at 300 K^{6,7}) in *Rb. sphaeroides*, considering that the effect of static disorder was not taken into account in the present calculation.

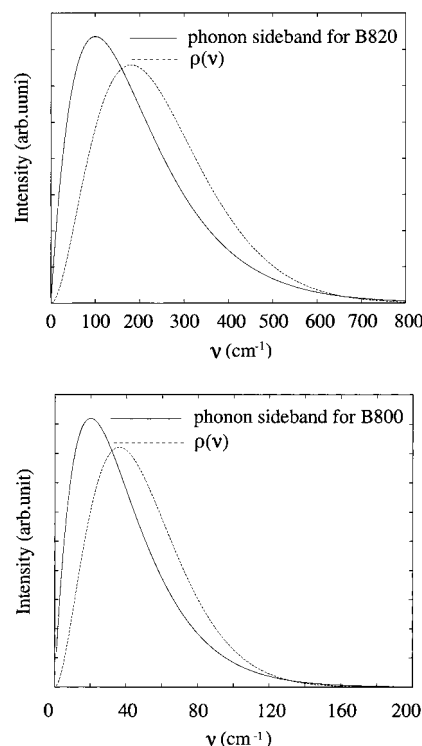


Figure 4. Phonon sideband spectrum $\Phi(\nu)$ and the weighted density of phonon states, $\rho(\nu)$, (a, top) for B850 and (b, bottom) for B800.

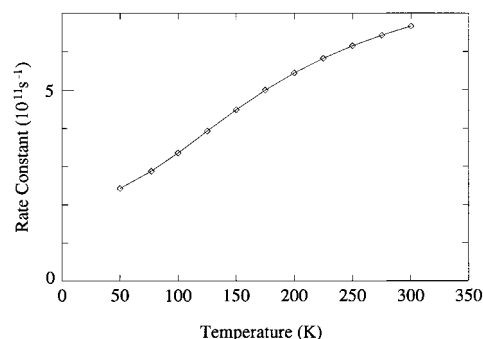


Figure 5. Rate constant of EET from B800 to B850 calculated as a function of temperature.

Figure 6 shows the luminescence spectrum $L^D(E)$ of B800 by a broken line, and $\sum_k I_k^A(E)$, the total density of states (DOS) of B850, by a solid line for 77 K (a) and 300 K (b). The largest overlap of $L^D(E)$ occurs with the fifth lowest peak ($k = \pm 4$) in the DOS of B850, contributing dominantly to the obtained EET rate constant, even though these states are optically forbidden. As temperature increases, exciton scattering by phonons becomes frequent and broadens both the DOS of B850 and $L^D(E)$. Since the peak of $L^D(E)$ does not coincide with a peak in the DOS of B850 in Figure 6, the overlap between them increases with temperature, leading to a larger rate constant at a higher temperature.

Although these results were obtained for a specific choice of parameters, the obtained EET rates are not sensitive to this choice. The positional interrelation between the B800 luminescence and the peaks in the B850 exciton DOS in Figure 6 changes when the parameters are changed. With this change, however, the EET rate is normally in the range of 10^{11} – 10^{12} s^{-1} with a temperature dependence similar to that in Figure 5, unless there is an accidental coincidence of the position of the B800 luminescence with a peak in the B850 exciton DOS. Changing our viewpoint, we notice the importance of this fact,

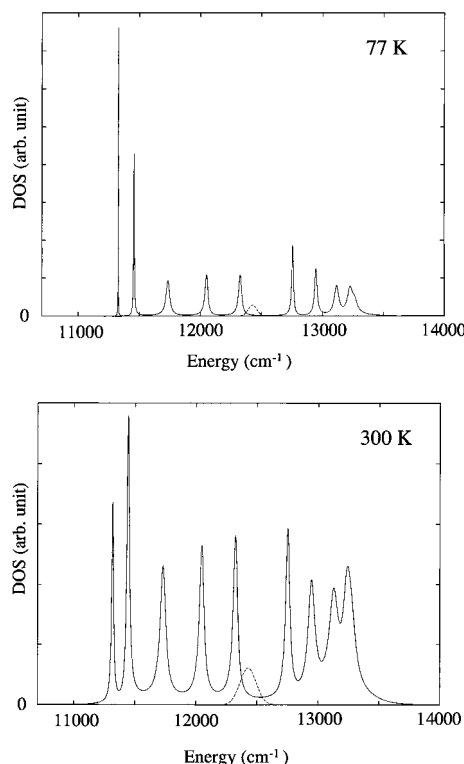


Figure 6. Density of exciton states in the B850 ring (solid line) and the luminescence spectrum of the B800 monomer (broken line) calculated (a) (top) at 77 K and (b) (bottom) at 300 K.

as shown below. EET can take place with a large rate to any optically forbidden exciton states in the B850 ring which are distributed with appreciable broadening and appropriate spacing in the exciton band as wide as about 2000 cm^{-1} . The EET from B800 is an example. This feature can be regarded as a strategy of the photosynthetic antenna for capturing excitation energies with a large rate at any position in the band. The present work has disclosed this strategy. On the other hand, this could not be disclosed by Förster's formula: For most values of the donor energy E , even if E is within the band, the rate constant of the EET would be brought about solely by a small overlap of the $L^D(E)$ with the second lowest (optically allowed) peak in the DOS of B850 in Figure 6. This would lead to a severe underestimation of the EET rate, for example, by several orders of magnitude for the EET from B800 as mentioned in the beginning.

4. Discussion

The very rapid EET from B800 to B850 in the LH2 complex has been a subject of hot discussions. Because it is not in accord with Förster's formula,^{7,35} various possibilities have been proposed.

One possibility is EET assisted by intramolecular vibrations of a BChl. In hole burning experiments,¹¹ satellite holes have been observed on the high-energy side of the B850 absorption band, being assigned as intramolecular vibration sidebands. Among them, the 750 cm^{-1} mode sideband was suggested to be responsible for the B800–B850 EET, since it drops in the same energy region as the B800 luminescence band. It has been clarified, however, that an unreasonably large exciton–phonon coupling would be required to explain the observed EET rate.¹² Furthermore, it has been argued recently that these satellite holes are unlikely to be of a vibronic origin.⁹

Another proposal is that the carotenoid molecule might be used as a virtual intermediate state for EET in a fourth-order

quantum mechanical process called the superexchange mechanism. Quantum chemical calculations have been carried out for the EET coupling between a BChl and a neurosporene (a simplified substitution for the carotenoid) in various intermolecular configurations.⁴⁰ A typical value of 1 meV ($\sim 8\text{ cm}^{-1}$) was obtained for the interaction between the lowest excited (S_1) state of neurosporene and the Q_y state of the BChl. This is too small to account for the observed B800–B850 EET rate by the superexchange mechanism, even if the S_1 state of the carotenoid lies closely above the B800 energy.

Another approach is the strong coupling (coherent-transfer) mechanism⁸ in which EET is assumed to occur much faster than reorganization of phonons around the donor and the acceptor. In this case the EET coupling directly gives a measure of the EET rate. Hu et al.²⁸ calculated systematically EET couplings relevant for the primary light-harvesting process, including those between the two LH2 rings, between LH2 and LH1, and between LH1 and the reaction center. Their calculation for the coupling between B850 and B800 in LH2 gave time constants of 390–530 fs. However, the strong coupling implies that the excitation energy must be transferred coherently back and forth between the donor and the acceptor. Such a coherent back transfer has not been observed in experiments. In contrast, our calculation is based on the weak coupling approach, which describes EET without coherent back transfer.

In conclusion, our calculation using the new formula of EET with reasonable exciton–phonon coupling explains the observed rapid EET qualitatively and semiquantitatively, without invoking any ad hoc assumptions unjustifiable from other experiments. The obtained large rate constants originate dominantly from EET between a B800 monomer and dipole-forbidden exciton states in B850. The present work has demonstrated that the proposed new formula of EET between molecular aggregates, eq 1, is suitable for the description of EET processes found in the antenna system of photosynthesis.

What has not been taken into account in the present work is the influence of static disorder. Its effect on the exciton states has been well studied by many investigators.^{7,18,23,41,42} The disorder broadens the peaks in the density of exciton states, and we expect that the temperature dependence of the EET rate become weaker. Such calculations are now under way and will be reported elsewhere.⁴³

Appendix: Self-Consistency Equation for the Self-Energy

The operator a_n in eq 10 is a linear combination of operator a_k 's which diagonalize the unperturbed exciton Hamiltonian H_e of eq 10 as in eq 14. Let us write this relation as

$$a_n = \sum_k \langle k|n \rangle a_k \quad (\text{A.1})$$

by introducing coefficient $\langle k|n \rangle$ for the linear combination. The self-energy for the exciton Green's function $G_k(E)$ can be calculated by the second equation in Figure 3. When eq A.1 and its Hermitian conjugate for a_n^\dagger are introduced to H' of eq 12, the interaction of an exciton at a site n with a phonon with energy ν_i contributes to the self-energy by an amount

$$S_i \nu_i |\langle k|n \rangle|^2 \sum_q |\langle q|n \rangle|^2 \left(\frac{n_i}{E - E_q + \nu_i + i\delta} + \frac{n_i + 1}{E - E_q - \nu_i + i\delta} \right) \quad (\text{A.2})$$

in the second-order approximation in the interaction, where n_i represents the thermal population of the phonon and δ represents a positive infinitesimal. This quantity should not depend on the site index n as long as n runs over either only odd or only even numbers, because the B850 ring has a rotational symmetry such that BChl dimer units are arranged.

Let us neglect, for simplicity, a small difference (or a small part in surplus of π) between BChl angles from the ring tangent within a dimer unit in the calculation of the self-energy. (This does not mean that we neglect the difference in BChl distances within a dimer unit and between adjacent dimer units. In fact, as the exciton energy spectrum E_k , we use that in Figure 2 obtained by taking full account of the differences in both angle and distance.) In this approximation for the self-energy, the environment around a BChl is regarded as the mirror image of that around the other BChl in a dimer unit. Therefore, the quantity in eq A.2 becomes independent of the site index n irrespective of whether n is an odd number or an even number, becoming completely independent of n . This nondependency on n results in that of $|\langle k|n\rangle|^2$ in eq A.2. Since the summation of $|\langle k|n\rangle|^2$ over all n 's is unity, this approximation leads us to

$$|\langle k|n\rangle|^2 = 1/2N \quad (\text{A.3})$$

since the total number of n 's is $2N$. Equation A.3 can be checked also by explicit calculation of $\langle k|n\rangle$, although it is omitted here.

Summation of the quantity in eq A.2 over all n 's and over all i 's gives the self-energy for the exciton Green's function $G_k(E)$ as

$$\Sigma(E) = \sum_i \frac{S_i \nu_i}{2N} \sum_q \left(\frac{n_i}{E + \nu_i - E_q + i\delta} + \frac{n_i + 1}{E - \nu_i - E_q + i\delta} \right) \quad (\text{A.4})$$

in the second-order approximation in the exciton-phonon interaction H' of eq 12. Here, the first term in parentheses on the right-hand side of eq A.4 results from the exciton scattering with one-phonon absorption, while the second term therein results from that with one-phonon emission.

As an approximation self-consistent with the self-energy of eq A.4, we consider that the zeroth-order Green's functions $(E + \nu_i - E_q + i\delta)^{-1}$ and $(E - \nu_i - E_q + i\delta)^{-1}$ appearing in eq A.4 should also have the same form of the self-energy, $\Sigma(E + \nu_i)$ and $\Sigma(E - \nu_i)$, respectively, as in eq 17. This corresponds to the procedure in the second equation in Figure 3. Accordingly, we are led to eq 18 as a self-consistency equation by which the self-energy $\Sigma(E)$ is determined as a function of the energy variable E .

References and Notes

- (1) As a review: Freisner, R. A.; Won, Y. *Biochim. Biophys. Acta* **1989**, 977, 99.
- (2) Deisenhofer, J.; Michel, H. *Annu. Rev. Biophys. Biophys. Chem.* **1991**, 20, 247.
- (3) McDermott, G.; Prince, S. M.; Freer, A. A.; Hawthornthwaite-Lawless, A. M.; Papiz, M. Z.; Cogdell, R. J.; Isaacs, N. W. *Nature* **1995**, 374, 517.
- (4) Koepke, J.; Hu, X.; Muenke, C.; Schulten, K.; Michel, H. *Structure* **1996**, 4, 581.
- (5) As a review: Hu, X.; Schulten, K. *Phys. Today* **1997**, 50(8), 28 and references therein.
- (6) Shreve, A. P.; Trautman, J. K.; Frank, H. A.; Owens, T. G.; Albrecht, A. C. *Biochim. Biophys. Acta* **1991**, 1058, 280.
- (7) Jimenez, R.; Dikshit, S. N.; Bradforth, S. E.; Fleming, G. R. *J. Phys. Chem.* **1996**, 100, 6825.
- (8) Förster, T. In *Modern Quantum Chemistry*; Sinanoglu, O., Ed.; Academic Press: New York, 1965; Vol. III, pp 93–137.
- (9) Wu, H.-M.; Ratsep, M.; Jankowiak, R.; Cogdell, R. J.; Small, G. J. *J. Phys. Chem. B* **1997**, 101, 7641.
- (10) De Caro, C.; Visschers, R. W.; van Grondelle, R.; Völker, S. J. *Phys. Chem.* **1994**, 98, 10584.
- (11) Reddy, N. R. S.; Small, G. J.; Seibert, M.; Picorel, R. *Chem. Phys. Lett.* **1991**, 181, 391.
- (12) Pullerits, T.; Hess, S.; Herek, J. L.; Sundström, V. *J. Phys. Chem. B* **1997**, 101, 10560.
- (13) Monshouwer, R.; de Zarate, I. O.; van Mourik, F.; van Grondelle, R. *Chem. Phys. Lett.* **1995**, 246, 341.
- (14) Sumi, H. *J. Phys. Chem. B* **1999**, 103, 252.
- (15) Fetisova, Z.; Freiberg, A.; Mauring, K.; Novoderezhkin, V.; Taisova, A.; Timpmann, K. *Biophys. J.* **1996**, 71, 995.
- (16) Prince, S. M.; Papiz, M. Z.; Freer, A. A.; McDermott, G.; Hawthornthwaite-Lawless, A. M.; Cogdell, R. J.; Isaacs, N. W. *Protein Data Bank* **1996**, 1KZU.
- (17) Sauer, K.; Cogdell, R. J.; Prince, S. M.; Freer, A.; Isaacs, N. W.; Scheer, H. *Photochem. Photobiol.* **1996**, 64, 564.
- (18) Alden, R. G.; Johnson, E.; Nagarajan, V.; Parson, W. W.; Law, C. J.; Cogdell, R. G. *J. Phys. Chem.* **1997**, 101, 4667.
- (19) Cory, M. G.; Zerner, M. C.; Hu, X.; Schulten, K. *J. Phys. Chem.* **1998**, 102, 7640.
- (20) Wu, H. M.; Reddy, N. R. S.; Small, G. J. *J. Phys. Chem. B* **1997**, 101, 651.
- (21) Nagarajan, V.; Alden, R. G.; Williams, J. C.; Parson, W. W. *Proc. Natl. Acad. Sci. U.S.A.* **1996**, 93, 13774.
- (22) Ritz, T.; Hu, X.; Damjanovic, A.; Schulten, K. *J. Lumin.* **1998**, 76–77, 310.
- (23) Barvik, I.; Warns, C.; Neidlinger, T.; Reineker, P. *Chem. Phys.* **1999**, 240, 173.
- (24) Monshouwer, R.; Baltuska, A.; van Mourik, F.; van Grondelle, R. *J. Phys. Chem. A* **1998**, 102, 4360.
- (25) Yu, J.-Y.; Nagasawa, Y.; van Grondelle, R.; Fleming, G. R. *Chem. Phys. Lett.* **1997**, 280, 404.
- (26) Chachisvilis, M.; Kuhm, O.; Pullerits, T.; Sundstrom, V. *J. Phys. Chem. B* **1997**, 101, 7275.
- (27) Jimenez, R.; van Mourik, F.; Yu, J.-Y.; Fleming, G. R. *J. Phys. Chem. B* **1997**, 101, 7350.
- (28) Hu, X.; Ritz, T.; Damjanovic, A.; Schulten, K. *J. Phys. Chem. B* **1997**, 101, 3854.
- (29) Reddy, N. R.; Cogdell, R. J.; Zhao, L.; Small, G. J. *Photochem. Photobiol.* **1993**, 57, 35.
- (30) Reddy, N. R.; Picorel, R.; Small, G. J. *J. Phys. Chem.* **1992**, 96, 6458.
- (31) van Dorssen, R. J.; Hunter, C. N.; van Grondelle, R.; Korenhof, A. H.; Ames, J. *Biochim. Biophys. Acta* **1988**, 932, 179.
- (32) Kramer, H. J. M.; Pennoyer, J. D.; van Grondelle, R.; Westerhuis, W. H. J.; Niederman, R. A.; Ames, J. *Biochim. Biophys. Acta* **1984**, 767, 335.
- (33) Nakajima, S.; Toyozawa, Y.; Abe, R. *The Physics of Elementary Excitations*; Springer-Verlag: 1980; Chapter 7, pp 263–319.
- (34) Hopfield, J. J. *Proc. Natl. Acad. Sci. U.S.A.* **1974**, 71, 3640.
- (35) Pullerits, T.; van Mourik, F.; Monshouwer, R.; Visschers, R. W.; van Grondelle, R. *J. Lumin.* **1994**, 58, 168.
- (36) Osad'ko, I. S. *Sov. Phys. Usp.* **1979**, 22, 311.
- (37) Kanematsu, Y.; Ahn, J. S.; Kushida, T. *Phys. Rev. B* **1993**, 48, 9066.
- (38) Kanematsu, Y.; Enomoto, M.; Nishikawa, Y.; Kushida, T.; Ahn, J. S. *J. Lumin.* **1995**, 64, 109.
- (39) Wu, H.-M.; Savikhin, S.; Reddy, N. R. S.; Jankowiak, R.; Cogdell, R. J.; Struve, W. S.; Small, G. J. *J. Phys. Chem.* **1996**, 100, 12022.
- (40) Nagae, H.; Kakitani, T.; Katoh, T.; Mimuro, M. *J. Chem. Phys.* **1993**, 98, 8012.
- (41) Freiberg, A.; Timpmann, K.; Lin, S.; Woodbury, N. W. *J. Phys. Chem. B* **1998**, 102, 10974.
- (42) Kumble, R.; Hochstrasser, R. M. *J. Chem. Phys.* **1998**, 109, 855.
- (43) Mukai, K.; Abe, S.; Sumi, H., to be submitted for publication.